JVST B
Journal of Vacuum Science & Technology B

Optical realization of the pascal—Characterization of two gas modulated refractometers

Cite as: J. Vac. Sci. Technol. B **39**, 044201 (2021); https://doi.org/10.1116/6.0001042
Submitted: 22 March 2021 . Accepted: 10 June 2021 . Published Online: 28 June 2021

Isak Silander, Clayton Forssén, Johan Zakrisson, Martin Zelan, and Ove Axner

JVST B
Journal of Vacuum Science & Technology B

ARTICLE

avs.scitation.org/journal/jvb

Optical realization of the pascal—Characterization of two gas modulated refractometers

Cite as: J. Vac. Sci. Technol. B 39, 044201 (2021); doi: 10.1116/6.0001042
Submitted: 22 March 2021 · Accepted: 10 June 2021 ·
Published Online: 28 June 2021

Isak Silander,[1] Clayton Forssén,[1,a)] Johan Zakrisson,[1] Martin Zelan,[2] and Ove Axner[1,b)]

AFFILIATIONS

[1]Department of Physics, Umeå University, SE-901 87 Umeå, Sweden
[2]Measurement Science and Technology, RISE Research Institutes of Sweden, SE-501 15 Borås, Sweden

[a)]**Also at:** Measurement Science and Technology, RISE Research Institutes of Sweden, SE-501 15 Borås, Sweden.
[b)]**Electronic mail:** ove.axner@umu.se

ABSTRACT

By measuring the refractivity and the temperature of a gas, its pressure can be calculated from fundamental principles. The most sensitive instruments are currently based on Fabry–Perot cavities where a laser is used to probe the frequency of a cavity mode. However, for best accuracy, the realization of such systems requires exceptional mechanical stability. Gas modulation refractometry (GAMOR) has previously demonstrated an impressive ability to mitigate the influence of fluctuations and drifts whereby it can provide high-precision (sub-ppm, i.e., sub-parts-per-million or sub-10^{-6}) assessment of gas refractivity and pressure. In this work, two independent GAMOR-based refractometers are individually characterized, compared to each other, and finally compared to a calibrated dead weight piston gauge with respect to their abilities to assess pressure in the 4–25 kPa range. The first system, referred to as the stationary optical pascal (SOP), uses a miniature fixed point gallium cell to measure the temperature. The second system, denoted the transportable optical pascal (TOP), relies on calibrated Pt-100 sensors. The expanded uncertainty for assessment of pressure ($k = 2$) was estimated to, for the SOP and TOP, $[(10\,\mathrm{mPa})^2 + (10 \times 10^{-6}\mathrm{P})^2]^{1/2}$ and $[(16\,\mathrm{mPa})^2 + (28 \times 10^{-6}\mathrm{P})^2]^{1/2}$, respectively. While the uncertainty of the SOP is mainly limited by the uncertainty in the molar polarizability of nitrogen (8 ppm), the uncertainty of the TOP is dominated by the temperature assessment (26 ppm). To verify the long-term stability, the systems were compared to each other over a period of 5 months. It was found that all measurements fell within the estimated expanded uncertainty ($k = 2$) for comparative measurements (27 ppm). This verified that the estimated error budget for the uncorrelated errors holds over this extensive period of time.

I. INTRODUCTION

In the SI-system of units, the pascal is defined as the force per unit area. In practice, it is realized with mechanical devices such as pressure balances and liquid manometers.[1–5] With the revision of the SI-system, an alternative path to realize the pascal has become feasible.[6,7] By measuring the refractivity and the temperature of a gas, it is possible to calculate its pressure by the use of the Lorentz–Lorenz equation and an equation of state.[8–12] Such a realization of the pascal does not depend on any mechanical actuator but instead measures directly on the gas, thereby potentially decreasing uncertainties and shortening calibration chains.

Work to realize the optical pascal takes place at multiple national metrological institutes and universities across the world. Some of the more prominent actors in this field are the National Institute of Standards and Technology (NIST), the National Institute of Metrology (NIM), the National Metrology Institute of Japan (NMIJ), the Physikalisch-Technische Bundesanstalt (PTB), the National Institute of Metrological Research (INRiM), the Laboratoire Commun de Métrologie (LNE-Cnam), the RISE Research Institute of Sweden, and Umeå University (UmU).[11–18] Substantial and concerted actions presently take place within the EMPIR initiative (the QuantumPascal project, No. 18SIB04).[19]

The most sensitive instruments are currently based on Fabry–Perot (FP) cavities where a laser is used to probe the frequency of a longitudinal mode.[20–25] The realization of such systems requires though an exceptional mechanical stability. For example, an uncertainty in the assessment of pressure of 2 mPa with a 15 cm long cavity requires a mechanical stability better than 1 pm. Despite

these challenges, such an instrument, based on an exceptionally well stabilized cavity, has demonstrated an impressive expanded uncertainty (k = 2) of $[(2.0\,\mathrm{mPa})^2 + (8.8 \times 10^{-6}\mathrm{P})^2]^{1/2}$.[25]

As a means to reduce the requirement of system stability and to improve on performance, the GAs MOdulation Refractometry (GAMOR) methodology has been developed. Refractometers encompassing this methodology have demonstrated impressive abilities to mitigate the influence of fluctuations and drifts,[26,27] whereby they have provided relaxed requirements on system stability. They have also demonstrated the highest precision to date.[28–30] This has opened up for cavity designs using alternative materials; pressure assessments with sub-ppm (sub-ppm, i.e., sub-parts-per-million or sub-10^{-6}) stability over 24 h have recently been demonstrated by the use of an Invar cavity.[18] The methodology has also allowed for the realization of transportable systems.[31,32]

While these instruments have impressive resolution, precision, and stability, the uncertainty has not until now been fully assessed. In this work, two refractometer instruments, both utilizing the GAMOR methodology, are characterized with respect to their expanded uncertainties when assessing pressure. The two systems are based on the same basic design. One of them is an upgraded version of a previously developed and characterized Invar-based refractometer that is built on a conventional optical table,[18] but for an improved assessment of temperature, it is equipped with a gallium fix point cell.[33] This system is in this work referred to as the stationary optical pascal (SOP). The other system has been constructed in a 19-in. rack and is not equipped with a gallium fix point cell; it assesses the temperature solely by the use of calibrated Pt-100 sensors.[32] Hence, this system, which can be seen as a transportable version of the SOP, is here referred to as the transportable optical pascal (TOP).

The two systems are in this work characterized with respect to their ability to realize the pascal by the use of N_2. The refractometers are first individually characterized, thereafter compared to each other, and finally compared to a calibrated dead weight piston gauge, which is also producing the pressure the refractometers are assessing.

The characterizations were performed by the use of the following procedures. First, all temperature probes in the two refractometers were calibrated with the help of the gallium fix point cell. Second, the cavity deformations of both refractometers were assessed by the use of the procedure presented in Ref. 34. Both refractometers were then individually characterized in the 4–25 kPa range. Comparison measurements were thereafter carried out by several series of assessments of the pressure produced by the piston gauge, performed over a period of 5 months. This provided possibilities to assess the degree of a long-term correlation between the pressure assessments of the two refractometers and between the refractometers and the piston gauge.

It was found that the expanded uncertainty for the SOP was $[(10\,\mathrm{mPa})^2 + (10 \times 10^{-6}\,\mathrm{P})^2]^{1/2}$, while that for the TOP was $[(16\,\mathrm{mPa})^2 + (28 \times 10^{-6}\,\mathrm{P})^2]^{1/2}$.

II. THEORY

A. Refractivity

Each refractometer is based on a dual-FP-cavity (DFPC) in which a laser is locked to each cavity, addressing the empty cavity modes q_{01} and q_{02} by the use of light whose frequencies are ν_{01} and ν_{02}, respectively. The beat frequency between the two lasers, f, is, at any time during the measurement, given by the difference between the two laser frequencies, i.e., by $|\nu_1 - \nu_2|$. For sufficiently large changes in pressure in the cavities, the frequencies of the lasers can no longer follow that of a given cavity mode, whereby the lasers will make automatic mode jumps. This implies that, as gas is let into the measurement cavity, f is a nonmonotonic (i.e., a wrapped) function. To take the mode jumps (denoted Δq_1 and Δq_2, counted from q_{01} and q_{02}, respectively) properly into account in the data evaluation, it has been found convenient to create an unwrapped (i.e., a mode-jump-corrected) beat frequency, f_{UW}, defined as

$$f_{UW} = \pm f - \left(\frac{\Delta q_1}{q_{01}}\nu_{01} - \frac{\Delta q_2}{q_{02}}\nu_{02}\right), \tag{1}$$

where the $\pm$ sign refers to the cases when $\nu_1 > \nu_2$ and $\nu_1 < \nu_2$, respectively.

The refractivity can then be conveniently expressed as a function of the shift of the unwrapped beat frequency, Δf_{UW}, defined as $f_{UW}(n) - f_{UW}(n = 1)$, and the relative cavity deformation, ε, which is given by $(\delta L/L_0)/(n-1)$, where δL and L_0 are the pressure induced length deformation and the empty cavity length, respectively.[28,29,35]

When cavity 1 is the measurement cavity, Δf_{UW} is negative, whereby the refractivity is given by

$$n - 1 = \frac{-\Delta f_{UW}/\nu_{01}}{1 + \Delta f_{UW}/\nu_{01} + \Delta q_1/q_{01} + \varepsilon}, \tag{2}$$

while when cavity 2 is the measurement cavity, Δf_{UW} is positive, whereby the refractivity is given by

$$n - 1 = \frac{\Delta f_{UW}/\nu_{02}}{1 - \Delta f_{UW}/\nu_{02} + \Delta q_2/q_{02} + \varepsilon}. \tag{3}$$

B. Molar density

For subatmospheric pressure, the molar density ρ can be calculated from the refractivity by the use of the extended Lorentz–Lorenz equation,

$$\rho = \frac{2}{3A_R}(n-1)[1 + b_{n-1}(n-1)], \tag{4}$$

where A_R and b_{n-1} are the molar dynamic polarizability and a series expansion coefficient, respectively. The latter is given by $-(1 + 4B_R/A_R^2)/6$, where, in turn, B_R is the second refractivity virial coefficient in the Lorentz–Lorenz equation.[8,29,35]

C. Pressure

For the same pressure range, the pressure can be obtained from the density and the temperature as

$$P = RT\rho[1 + B_\rho(T)\rho], \tag{5}$$

TABLE I. Gas coefficients for N_2 at 302.91 K and 1550.14 nm.

Coefficients	Value (k = 2)	Reference
A_R	$4.396549(34) \times 10^{-6}$ m^3/mol	34 and 36
b_{n-1}	−0.195(7)	25 and 34
B_ρ	$-4.00(24) \times 10^{-6}$ m^3/mol	34 and 36

where R is the molar gas constant, T is the temperature of the gas, and $B_\rho(T)$ is the second density virial coefficient.[11,12]

D. Molecular data

In this work, the two refractometers are characterized with respect to their ability to assess the pressure of nitrogen. Table I provides information about the relevant gas constants for nitrogen, A_R, b_{n-1}, and B_ρ, at the temperature and wavelength used (302.91 K and 1550.14 nm, respectively).

E. Set pressure of the piston gauge

The set pressure of the piston gauge, P_{PG}, is calculated as

$$P_{PG} = \frac{(m_p + \sum_i m_i)g \times cos(\theta)}{A_{eff}[1 + \alpha(T_p - T_{ref})]} + P_{hood}, \quad (6)$$

where m_p is the mass of the piston, m_i is the individual mass placed on the piston, g is the local gravity, θ is the piston cylinder assembly angle with respect to the gravity vector, A_{eff} is the effective area of the piston at the pertinent temperature, T_{ref}, α is the combined temperature expansion of the piston and cylinder, T_p is the measured temperature, and P_{hood} is the hood pressure.

To be able to accurately relate the pressures of the various systems to each other, their differences in height with respect to a given reference plane must be taken into account. This was done by using the expression

$$\Delta P_h = \rho_m g \Delta h, \quad (7)$$

where ρ_m is the mass density of the gas under investigation and Δh is the difference in height with respect to a reference plane. We estimate the density to be proportional to the pressure and add a correction term of 109.5 ppm/m to all nitrogen measurements.

III. EXPERIMENTAL SETUP

The experimental setup, shown in Fig. 1, consists of two GAMOR-based refractometers, the SOP and the TOP, that are connected to a dead weight piston gauge (RUSKA 2465A) by the use of a gas supply and evacuation system.

A. Refractometers

The refractometers, which comprise Invar-based DFPCs with free-spectral-ranges (FSRs) of 1 GHz and finesse values of 10^4, which thus have cavity modes with a full-width-half-maximum of 100 kHz, that are addressed by Er-doped fiber lasers emitting light within the C34 communication channel, i.e., around 1.55 m, are

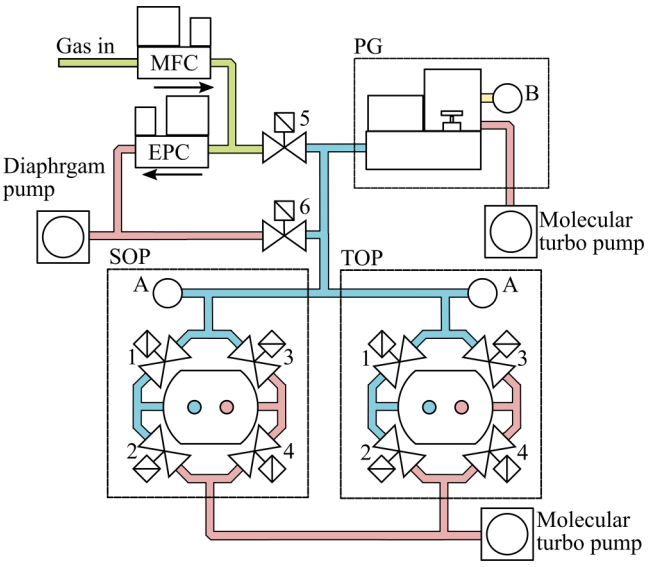

FIG. 1. Schematic illustration of the experimental setup. The two refractometers, the SOP and the TOP, are connected to the same pressure inlet and evacuation systems (shown with green and red colors, respectively). The pressure assessed is produced and regulated by a common piston gauge. The part of the system whose pressure is assessed is shown in blue. MFC, mass flow controller; EPC, electronic pressure controller; PG, piston gauge; A and B, pressure gauges; and 1–6, valves. See the text for details.

described in more detail in Refs. 18 and 33. They are equipped with an automatic relocking routine that ensures that the lasers make a controlled mode hop when their frequencies have changed one FSR. The cavity mode numbers are continuously monitored and unambiguously assessed by the use of the laser feedback voltages and the pressure gauges.

B. Temperature regulation and assessment

For best accuracy, the temperatures of the refractometers were held close to the melting point of gallium (29.76°C). The temperatures were stabilized in two steps. First, the breadboard onto which the optics and the cavity oven were mounted was stabilized within 10 mK of this melting point. The temperature of the oven (in which the Invar cavity was mounted) was then stabilized; therefore, the temperature of the cavity spacer, measured by the use of three Pt-100 probes bored into the spacer, was within 1 mK of the set temperature. To stabilize also the gas handling system, the valves 1–4 were mounted on top of the oven. Before the measurement campaign, the Pt-100 cavity probes were calibrated with respect to a gallium fixed point cell. Since the system was used close to the fixed point of gallium, this was found adequate.

However, the assessment of the temperature with the Pt-100s can drift over time, adversely affecting their ability to accurately assess the temperatures of the cavities. To alleviate this, we recently developed an automated gallium fix point cell, working around the melting point of gallium.[37] The temperature of the SOP cavity

spacer was then assessed also by the use of a thermocouple referred to this gallium fix point cell.[33] By this, the expanded uncertainty of the temperature of the cavity spacer (k = 2) was estimated to be 1.2 mK.

C. Gas system

The gas is controlled by a set of ten valves (Swagelok, 6LVV-DPFR4-P-C) comprising two sets of four gas modulation valves (denoted 1–4 in the SOP and the TOP in Fig. 1), one gas fill valve (marked 5), and a pump down valve (6). The "high" pressure side of the refractometer is evacuated by the use of a diaphragm pump, while the two refractometers are evacuated by the use of a common molecular turbo pump. The hood is constantly evacuated by a separate molecular turbo pump.

The pressure is monitored by a set of pressure gauges denoted A or B. A represents a pair of pressure gauges (Oerlikon-Leybold, CTR 101 N 1000 Torr) used to monitor the high pressure side of the refractometers, while B denotes the pressure gauge used to monitor the hood pressure (Oerlikon-Leybold, ITR90).

The gas modulation is achieved by switching the valves between two states. State I, the gas filling state, is initiated by opening valves 1 and 4 (while valves 2 and 3 are closed), whereby cavity 1 is filled with gas while cavity 2 is evacuated. The length of this state is chosen so that the assessed pressure in the measurement cavity stabilizes well to that provided by the piston gauge (50 s). In state II, the evacuation state, valves 2, 4, and 6 are open while valve 1 is closed, whereby both cavities are being evacuated (50 s). Valve 3 is constantly closed. Valves 1–4 and 6 are controlled through a digital output module (National Instruments, NI-9474), while valve 5 is controlled by the switching relay in the vacuum gauge controller (Leybold, Graphix three).

The result of this scheme is that in state I, the gas will flow through valve 5 into the piston gauge and the high pressure side of the refractometer until the pressure measured by gauge A exceeds the set pressure of the piston gauge. At this point, valve 5 will close. As a result of this, the piston in the piston gauge will rise, setting the pressure in the system to that produced by the piston gauge. The piston will float for the rest of state I, while the gas from the MFC will flow through the EPC so as to avoid the build up of contamination on the high pressure side of valve 5.

Valve 5 will reopen in state II when the pressure assessed by gauge A drops 10% of the set pressure of the piston gauge. To flush the "high" pressure side of the refractometer in state II, the gas flows through the MFC, valve 5, and out through valve 6.

D. Piston gauge

To ensure minimum friction between the piston and cylinder, the piston was rotating during the gas filling part of the modulation cycle. This was achieved by adding a timed relay to the cylinder rotation motor that is triggered by the closing of valve 5. This results in a combined rotation of the piston and cylinder during 10 s. The cylinder was thereafter stopped, whereby the piston, due to its finite inertia, continues to rotate freely through the measurement phase of the cycle.

E. Data acquisition

All data were evaluated by the use of the interpolation methodology that is a part of the GAMOR methodology.[28,29] The shift in the beat frequency, Δf_{UW}, was taken as the difference between the mean value of the unwrapped beat frequency, f, measured over the last 10 s of state I (i.e., with gas in the measurement cavity and rotating piston) and the interpolated value of two empty cavity beat frequency measurements (state II), each averaged over 5 s.

By the procedures described above, the system could work autonomously and unattended for any amount of time. The only time when human interference was needed was when the weight of the piston gauge or the gas had to be changed.

IV. RESULTS

The measurements presented here were taken during a measurement campaign spanning five months, from October 2020 to February 2021.

A. Refractometry characterizations

1. Cavity deformations

A procedure for low uncertainty assessment of cavity deformation, based on two high-purity gases (helium and nitrogen) and a high-precision refractometer, was recently presented by the authors.[34] It was demonstrated that the deformation of the cavity addressed could, when a GAMOR-based instrumentation was used, be assessed with an expanded uncertainty (k = 2), which is a fraction of the uncertainty of the molar polarizability of nitrogen, viz., 1 ppm.

The cavity deformations of the two Invar cavities were, therefore, assessed by the use of this procedure. The measurement data from the cavity characterizations are presented in Fig. 2. The cavity deformation parameters for nitrogen (ε) were found to be 0.001972 (1) and 0.001927(1) for the SOP and TOP, respectively. Since $(n-1) \propto (1-\varepsilon)$, as indicated in Table II, the measurement uncertainty in the cavity deformations will contribute to the total expanded uncertainty in pressure (k = 2) with 1 ppm.[38]

2. Laser frequencies

The measurement campaign was started by assessment of the frequencies of the two lasers when locked to evacuated cavities, i.e., ν_{01} and ν_{02}. By the use of a wavemeter (Burleigh, WA-1500), these were assessed with a relative uncertainty of 0.2 ppm.

3. Mirror dispersion

Since laser light with wavelengths in the commonly used communication band around 1.55 m is used and there are a multitude of mirrors being produced that have a minimum of dispersion (virtually no linear dispersion) at this wavelength, there is no significant influence of mirror dispersion on the cavity modes. This implies that the FSR is frequency independent, which, in turn, implies that the influence of a mode jump on the assessment of refractivity can, for cavity i, be assessed as $\Delta q_i \nu_{0i}/q_{0i}$, as stated in Eq. (1).

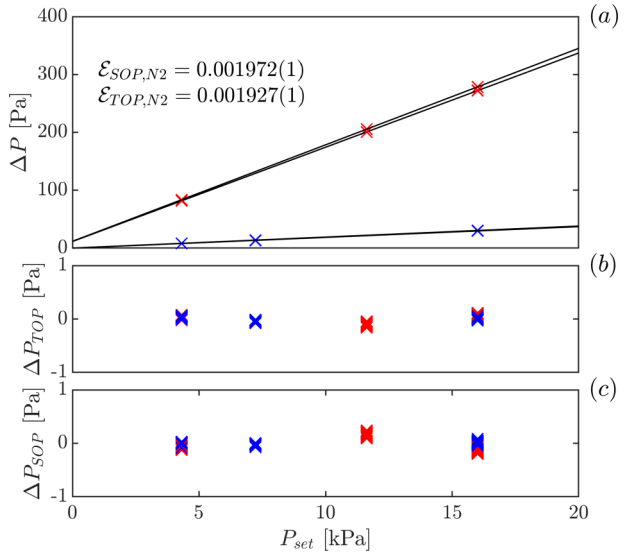

FIG. 2. Measurements from the characterization of the cavity deformations. The ΔP in panel (a) represents the difference between the pressure assessed by the refractometers by the use of Eqs. (1)–(6) with ε being zero and the set pressure of the piston gauge, as given by Eq. (7). The ΔP_{TOP} and ΔP_{SOP} in panels (b) and (c), respectively, represent the difference between the ΔP in panel (a) and the linear fits. In all panels, red markers represent helium measurements and blue markers represent nitrogen measurements. The cavity deformations for the SOP and TOP were found to be (for nitrogen) 0.001972(1) and 0.001927(1), respectively.

4. Cavity mode numbers

The cavity mode numbers, i.e., q_{01} and q_{02}, were determined with no uncertainty as the closest integer to the ratio between the laser frequency and the FSR of the cavity. The assessed mode numbers were verified by ensuring that the assessed refractivity (or pressure) is a continuous function when the lasers are making (controlled) mode jumps. For the measurement cavity of the SOP, the FSR and q_{01} were assessed to 1.012 597 GHz and 190 995, respectively. For the TOP, they were assessed to 1.012 479 GHz and 191 008, respectively.

5. Long-term stability

The long-term stability of the system was estimated by repeated system characterizations during the 5 month long measurement campaign. It was found that the empty cavity mode numbers q_{01} and q_{02}, for both the SOP and TOP, remained unchanged throughout the entire campaign, while the ν_{01} and ν_{02} drifted slowly within the mode hop free range of $\pm$ half an FSR (thus not giving rise to any undetected changes of the empty cavity mode numbers). This is an indication of the high stability of the cavity and laser system. It was estimated, from a set of repeated assessments of ν_{01} and ν_{02} taken between the periods of characterization, that this drift contributes to the expanded uncertainty in the assessment of pressure (k = 2) of 3 ppm.

TABLE II. Uncertainty budget of the pressure assessments by the use of the SOP [$U(P_{SOP})$] and the TOP [$U(P_{TOP})$]. All uncertainties are given as k = 2. The uncertainties of the b_{n-1}, $B_p(T)$, and the pressure-volume (PV) work are given for the highest pressure addressed (25 kPa).

Components	U_{SOP}	U_{TOP}	Type
Constant terms			
Empty cavity repeatability, Δf	7 mPa	11 mPa	A
Outgassing and leaks, A_R	5 mPa	11 mPa	A
Residual pressure, P	5 mPa	5 mPa	A
Linear terms			
Molar polarizability, A_R	8 ppm	8 ppm	B
Temperature assessment, T	4 ppm	26 ppm	B/A
Laser frequency, ν_0	3 ppm	3 ppm	A
Cavity deformation, ε	1 ppm	1 ppm	A
Gas purity (N_2), A_R	0.6 ppm	0.6 ppm	B
Quadratic terms (@25 kPa)			
b_{n-1} in Eq. (4), B_R	0.5 ppm	0.5 ppm	B
$B_p(T)$ in Eq. (5), $B_p(T)$	3 ppm	3 ppm	B
PV work, T	2 ppm	2 ppm	A
Total: $U(P_{SOP})$	$[(10\ \text{mPa})^2 + (10 \times 10^{-6}\ P)^2]^{1/2}$		
Total: $U(P_{TOP})$	$[(16\ \text{mPa})^2 + (28 \times 10^{-6}\ P)^2]^{1/2}$		

6. Gas constants

Although the molar polarizability of helium is known with low (sub-ppm) uncertainty through *ab initio* calculations,[39] the molar polarizability of nitrogen has so far been experimentally assessed by Egan *et al.* solely with an expanded uncertainty (k = 2) of 6.7 ppm; it was assessed to 4.446139 (30) $\times$ 10^{-6} cm^3/mol at a temperature of 302.919 K and a wavelength of 633 nm.[11,25] To be useful for assessment of nitrogen for the Invar-based GAMOR system, this value has to be scaled from the temperature and wavelength at which it was assessed to the ones that are used by this system, viz., 302.915 K and 1.55 m.

As can be concluded from Sec. 4.2 of the supplementary material to the work by Zakrisson *et al.*,[34] the small difference in temperature (4 mK) has neither any significant effect on the aforementioned value of the molar polarizability of nitrogen nor on its uncertainty.

The wavelength used in this work (1.55 m) differs though markedly from that used by Egan *et al.* Zakrisson *et al.* have, in Sec. 4.3 of the supplementary material to their work,[34] derived a methodology that, based on assessments of the refractivity at two dissimilar wavelengths, can provide a wavelength shifted value of the molar polarizability of nitrogen at one wavelength in terms of that of another.

Peck and Khanna have assessed refractivity values for nitrogen over a range of wavelengths.[40] Although they state that all their data could possibly be off by a common value ("The internal precision of the data is considered to be some two orders of magnitude better than that of the absolute value."), the relative rms uncertainty of their fit to their data, and thereby their assessment of the dispersion of nitrogen, is extraordinarily low, solely 2.6 ppm (given by $0.075 \times 10^{-8}/28352 \times 10^{-8}$). This implies that their data can be used for the aforementioned scaling. Utilization of their data shows that the molar polarizability of nitrogen at 1.55 m can be related to that at 633 nm as $A_{R,N_2,1.55\,\mu m} = 0.988\,851\, A_{R,N_2,633\,nm}$.[34] Using the

aforementioned value for $A_{R,N_2,633\,nm}$ assessed by Egan *et al.*, this implies that an adequate value of $A_{R,N_2,1.55\,\mu m}$ for the Invar-based GAMOR system presented here is $4.396\,569 \times 10^{-6}$ cm^3/mol.

The uncertainty of this value can be considered to originate from three sources, viz., the uncertainty in the dispersion of nitrogen assessed by Peck and Khanna, the influence of the offset in their assessments, and the difference in the second order refractive virial coefficients at the two wavelengths.

It is plausible to assume that the uncertainty in the dispersion of nitrogen assessed by Peck and Khanna is limited to the relative rms uncertainty of their fit, i.e., to 2.6 ppm. Section 4.3 of the supplementary material to the work by Zakrisson *et al.*[34] shows that the influence of the offset in their assessments can be assumed to contribute to the uncertainty in the molecular polarizability of nitrogen by up to 2.5 ppm, while the uncertainty of the difference in the second order refractive virial coefficients contribute solely with 0.78 ppm.

Summing all these uncertainties in quadrature provides a value of 7.6 ppm, which here is rounded off upward to 8 ppm.

The virial coefficients, B_R and $B_\rho(T)$, are not known with the same degree of accuracy as A_R. On the other hand, the nonlinear terms in the Lorentz–Lorenz equation and the equation of state that comprise these play a successively smaller role in the assessment of pressure the lower the pressure. They contribute to the uncertainty budget of the pressure assessment by 0.02 and 0.13 ppm/kPa, respectively. Hence, they play a minor role for the pressures addressed in this work. The values given in Table II, 0.5 and 3 ppm, respectively, are for the highest pressure addressed in this work (25 kPa).

7. Gas purity (nitrogen)

Any impurity in the N_2 will affect the assessments of pressure. This gas was taken from a university central system, in which the gas is produced from a supply of liquid nitrogen. A trace gas analysis of this gas (performed 2019) revealed that it contained 2 ppm H_2O and 1.6 ppm O_2. Since the refractivity of these two constituents differs from that of N_2 by 10% and 25%, it was assumed that impurities in the gas supply of N_2 can contribute to an expanded uncertainty in the assessment of pressure ($k = 2$) of 0.6 ppm. The fact that this uncertainty was significantly below those of the total system was verified by pressure assessments of N_2 made on 6N N_2 from a gas cylinder. No detectable difference between assessments of pressure using the two different sources of N_2 was observed.

8. Temperature assessments

The expanded uncertainty of the temperature assessment of the cavity spacer in the SOP, assessed by the thermocouple with respect to the gallium fixed point cell ($k = 2$), was estimated to 1.2 mK (4 ppm).[33]

By the use of this system, it was possible to estimate the stability of the Pt-100 temperature assessment in the SOP by a comparison of the two temperature assessment systems. The uncertainty in the temperature assessment of the Pt-100 sensors was estimated as the sum of the root-mean-square of the difference in the measured temperature by the two systems over 10 melting cycles (≈40 days) and the uncertainty in the assessed temperature of the combined thermocouple and gallium cell (i.e., assuming they are correlated). The expanded uncertainty in the temperature assessment by the Pt-100 ($k = 2$) was assessed to 7.8 mK (26 ppm). Although this assessment was done for the Pt-100s in the SOP, it was assumed that the Pt-100 measurements in the TOP had the same uncertainty.

9. PV work

When gas is let into an empty volume, the gas molecules can gain an amount of energy that is up to the product of the pressure and the volume (PV).[41,42] When the molecules have passed the valve, this energy will be transferred, by collisions, to the walls of the subsequent tubing and the cavity, which thus will be heated.

When this volume is emptied (pumped out), the molecules will, in turn, carry this energy with them from the walls of the tubing and cavity, which, therefore, will be cooled. The net amount of energy gained/lost by a complete gas modulation cycle is thus expected to be virtually zero.

The error associated with PV work will be given by the temperature difference between the gas in the center of the cavity and that of the temperature probes. If the modulation cycle is substantially longer than the time it takes for thermalization of the system, there will be no such temperature difference. As will be shown in an upcoming work by Rubin *et al.*,[43] the limiting factor for thermalization will be the dissipation of energy from the cavity wall into the spacer, resulting in an exponential decline of the temperature of the gas with a time constant that is less than 10 s.

In addition, given the small volume in the Invar-based GAMOR system (5 cm^3) and that the pressures addressed are restricted (≤30 kPa), each gas filling brings solely in a small amount of energy (≤0.15 J) into the measurement cavity. Hence, at the time for the acquisition of data (which is after 40 s when 100 s long cycles are used), the temperature assessed is, for all practical purposes, that of the gas. The simulations indicate that the contribution of the PV work to the total expanded uncertainty ($k = 2$) is below the ppm level.[43]

This conclusion is largely supported by data taken continuously during a 200 s long gas filling cycle. Figure 3 shows that, from the time when the pressure has settled to such a value that its value is within the scale of the figure, which takes place after ≈18 s, the assessed pressure drifts less than 2 ppm over the remaining 80 s (the dashed horizontal lines correspond to ±3 ppm). To allow for any unforeseen processes not accounted for in the simulations, we estimate the total expanded uncertainty ($k = 2$) due to PV work to be 2 ppm.

10. Empty cavity repeatability

The precision of the system was evaluated by empty cavity measurements, performed as a series of measurements with both cavities continuously pumped down (i.e., with valves 2 and 4 constantly open). Six hours of data, analyzed as if the gas in the measurement cavity were modulated, is presented as the measurement series (i) in Fig. 4. In agreement with the previous empty cavity assessment by the use of the GAMOR methodology,[18] the system does not show any drifts on this scale, only stochastic noise. The standard deviations of this noise, which predominantly originate from cavity and laser fluctuations, were, for the SOP and TOP, assessed to (over 6 h) 7 and 11 mPa ($k = 2$), respectively (which

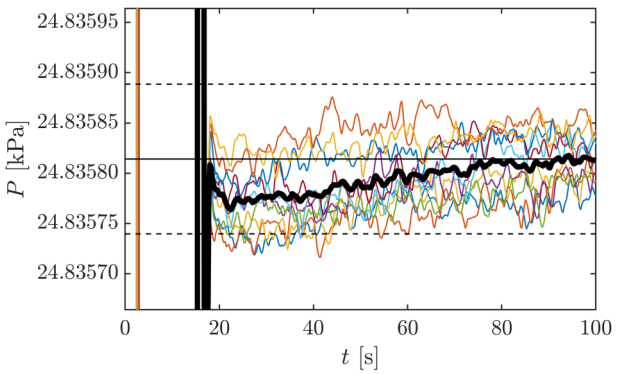

FIG. 3. Cycle-resolved pressure assessments by the SOT. To visualize the temperature equilibration processes in the system, gas modulation cycles with a length of 200 s were used. The figure shows, by the colored curves, the 100 s long gas filling state of ten such cycle-resolved assessments of pressure in the SOP at a pressure of 25 kPa. The thick black line displays their average. Dashed horizontal lines: ±3 ppm from the mean evaluated pressure. For the first 18 s, the assessed pressure is mainly outside the scale of the plot.

correspond to fluctuations of the beat frequencies of less than 4 and 6 kHz, respectively).

11. Outgassing and leaks

To estimate the influences of outgassing and leaks in the system, measurements were performed with no filling or flushing of the system (i.e., with valves 5 and 6 closed), with valve 4 constantly open, while valves 1 and 2 were alternatively open and closed (as in ordinary GAMOR). The first six hours of data taken after a change of weight in the piston gauge (thus after when the hood compartment of the piston gauge has been exposed to ambient air) is presented as the measurement series (ii) in Fig. 4. The first part of the data shows a decreasing signal that levels off within a few hours. This initial signal is attributed to the exposure of the piston gauge to ambient air. After a couple of hours of stabilization (with repeated evacuating empty cavity assessments), the background signal in the system was found to settle to 30 and 70 mPa for the SOP and the TOP, respectively (assuming the gas is nitrogen). Since the cavity filling process extracts 5 cm^3 of gas once per gas cycle (100 s), this corresponds to outgassing and leaking rates of 0.6 and 1.4 × 10^{-12} mol/s, respectively.

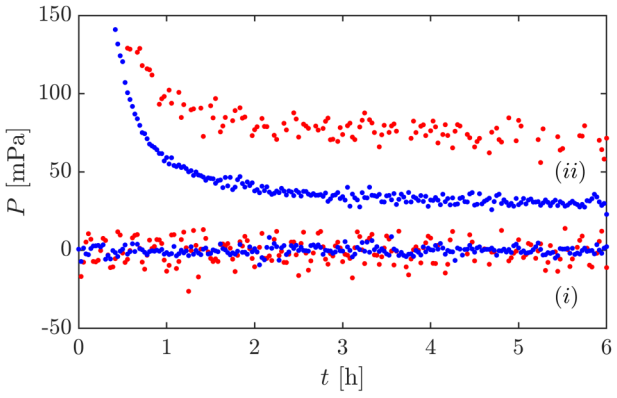

FIG. 4. Zero measurements without gas filling (i.e., with valves 5 and 6 closed) during the first six hours after a change of weight in the piston gauge. Curves (i) with continuous pumping (i.e., with valve 2 continuously open), thus showing the precision of the system. Curves (ii) with valves 1 and 2 alternatively open and closed (as in ordinary GAMOR measurement procedures), thus indicating the amount of outgassing and leaks in the system. Blue markers: the SOP; red markers: the TOP.

When pressure is assessed, however, the actual influence of these processes on the evaluated pressure is solely a fraction of this, given by the relative difference in refractivity of the outgassed (or leaked) gas and the gas addressed (nitrogen). Since the most common contaminants, e.g., water, air, and oxygen, have refractivities that differ from that of N_2 by less than 13% [it is basically only hydrogen that has a refractivity that differs markedly from that of N_2 (44%)], it is feasible to assume that outgassing and leaks will not add to the total uncertainty with more than a fraction of the settling pressures, viz., 5 and 11 mPa. The difference in the two values is currently attributed to different lengths of gas lines in the two systems.

12. Residual pressure

The refractometers effectively assess the difference in refractivity between the filled measurement cavities and the reference cavities. Any residual pressure in the reference cavities will, therefore, affect the assessments. The residual pressure in the gas line to the turbo was found to be less than 5 mPa. As the refractometer signals are affected by the residual pressure in the gas line, the errors from a residual pressure in the reference cavities are likewise assumed to be smaller than 5 mPa.

13. Total expanded uncertainty

The total expanded uncertainty can be calculated by combining all of the entities above. As is presented as the last two lines in Table II, it was found that the expanded uncertainty (k = 2) for the SOP (using the gallium fix point cell) was $[(10\,\text{mPa})^2 + (10 \times 10^{-6}\,\text{P})^2]^{1/2}$ while that for the TOP (which assesses the temperature by the Pt-100 sensors) was $[(16\,\text{mPa})^2 + (28 \times 10^{-6}\,\text{P})^2]^{1/2}$. The difference in the constant term stems from the difference in outgassing and leaks in Fig. 4, while that in the linear dependence originates from a larger uncertainty in the temperature assessments of the TOP.

B. Comparison of the two refractometers—The SOP vs the TOP

To assess the long-term stability and the degree of concordance of the two refractometers, a series of measurements was taken over a five-month period, each comprising a set of pressures (up to 25 kPa) produced by the piston gauge (thus for a set of weights). To reduce the disturbance, an opening of the piston

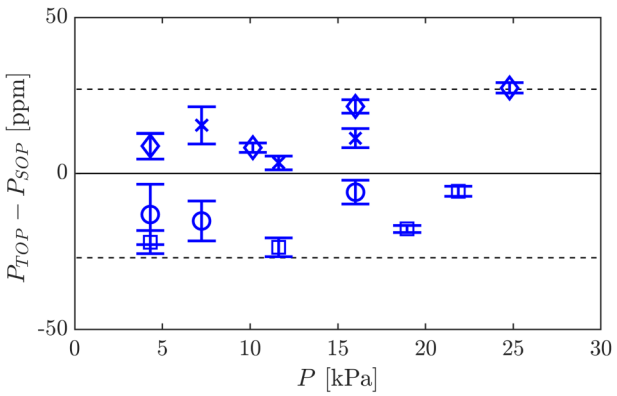

FIG. 5. Difference in pressure measured by the TOP and SOP, defined as $P_{TOP}-P_{SOP}$, for a series of measurements taken during a period of 5 months (taken in October, November, December, and February, represented by crosses, circles, squares, and diamonds, respectively). Each weight was measured over 24 h with the pressure assessed as the mean of the last 50 modulation cycles (thus over 1.4 h). The error bars represent a two standard deviation spread over these points. The dashed lines represent the estimated uncertainty (k = 2) from the uncorrelated sources of uncertainty (i.e., the temperature assessment, the laser wavelength, the repeatability, and the zero pressure).

gauge hood can give rise to (exemplified by the first part of the data sets (ii) in Fig. 4), each weight was measured over 24 h, while the pressure was assessed solely as the mean of the last 50 modulation cycles (thus over the last 1.4 h).

Figure 5 shows the difference between the assessed pressure from the SOP and TOP as a function of pressure. The data comprise four sets of measurements, taken during the months of October, November, December (2020), and February (2021), represented by crosses, circles, squares, and diamonds, respectively. The error bars represent two standard deviations of the spread of the data.

The expanded uncertainty of this difference (k = 2) was estimated from the uncorrelated sources of uncertainty, i.e., from the laser frequency, the temperature assessment, the repeatability, and the residual pressure, to 27 ppm. This uncertainty is illustrated by the black horizontal dashed lines in Fig. 5. The figure shows that all data points taken over the five-month long measurement campaign are within the estimated uncertainty. This verifies that the error budgets for the uncorrelated errors given above hold over this time period. It can also be seen that the spread within each set of measurements (crosses, circles, squares, and diamonds) is considerably smaller than the spread of the entire set of data. This is mainly attributed to drifts of the Pt-100 modules assessing the temperature in the TOP.

C. Comparison of the refractometers with the piston gauge

The two refractometers were also compared with the set pressure of the piston gauge.

TABLE III. Expanded uncertainty components of the pressure set by the piston gauge, $U(P_{PG})$. All expanded uncertainties are expressed as k = 2.

Uncertainty components	u_{PG}	Type
Constant terms		
Hood pressure, P_{hood}	50 mPa	A
Mass, $m_p + \sum m_i$	31 mPa	B
Linear terms		
Piston area, A_{eff}	34 ppm	B
Temperature expansion, α	17 ppm	B
Horizontal level, θ	13 ppm	B
Local gravity, g	3 ppm	B
Sum: $U(P_{PG})$	$[(60\ \text{mPa})^2 + (41 \times 10^{-6}\ \text{P})^2]^{1/2}$	

1. Uncertainty of the piston gauge

The pressure of the piston gauge is estimated by the use of Eq. (6). The components contributing to its expanded uncertainty, which are given in Table III, were estimated as follows.

The effective piston area A_{eff}, the piston mass m_p, and the individual masses m_i have all recently been calibrated at RISE (calibration protocols 105102-2P00494-K11, 105102-2P00494-K08, and 105102-2P00494-K09). The uncertainty in the effective piston area A_{eff} was assessed to 34 ppm. The uncertainties of the masses used for each individual set pressure were summed (i.e., assuming they were correlated). The largest of these (31 mPa) was taken as the mass uncertainty. The thermal coefficient α of the effective area of the piston was taken from the user manual (15 ppm/K). Its accuracy is here estimated (by the use of a rectangular distribution) to be 10% of this value. As the system was operating close to 29.76 °C, this contributes to the expanded uncertainty (k = 2) from the temperature dependence of the effective piston area with an amount of 17 ppm. The hood pressure was continuously monitored and corrected for. Its uncertainty was taken as 20% of the largest hood pressure recorded (which was 250 mPa). The value for the local gravity was calculated by an interpolation from surrounding gravity observations using a remove-interpolate-restore technique by The Swedish Mapping, Cadastral and Land Registration Authority (swe. Lantmäteriet). The piston cylinder assembly was leveled with the help of a bull's eye level placed on the piston before the measurement. The accuracy of this method was estimated to be 0.3°, which provides a contribution to the error budget of 13 ppm.

The total expanded uncertainty of the piston gauge (k = 2), $U(P_{PG})$, was calculated by combining all of the entities above. As is shown by the last line of Table III, it was estimated to $[(60\ \text{mPa})^2 + (41 \times 10^{-6}\ \text{P})^2]^{1/2}$.

It is interesting to note that the total expanded uncertainties of both refractometers are smaller than that of the piston gauge.

2. Comparison with the piston gauge

Figure 6 shows the difference between the assessments of the two refractometers and the set pressures of the piston gauge taken during the last two measurement series (December and February) as a function of piston gauge set pressure. The assessment made by

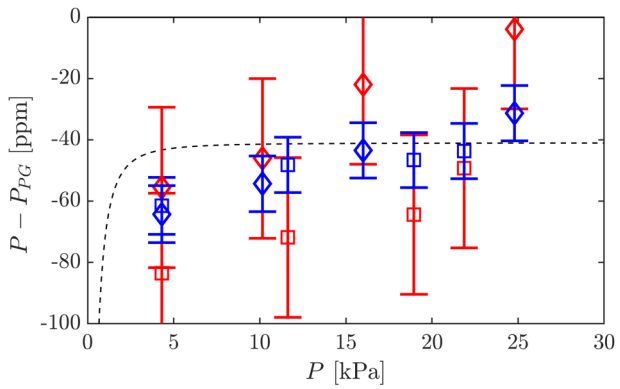

FIG. 6. Difference between two series of pressures measured by the refractometers and the set pressure of the piston gauge taken over 3 months (one in December 2020 and one in February 2021, represented by squares and diamonds, respectively). Blue markers: $P_{SOP}-P_{PG}$. Red markers: $P_{TOP}-P_{PG}$. The error bars represent the expanded uncertainty of the pressure (k = 2) assessed for the SOP as $U(P_{SOP})$ and the TOP as $U(P_{TOP})$. The dashed lines represent the (k = 2) uncertainty of the piston gauge $U(P_{PG})$.

the SOP and the TOP is given by the blue and red markers, respectively. The error bars of the individual data points represent the expanded uncertainties (k = 2) of the pressure assessed by the refractometers, i.e., for the SOP and TOP, $U(P_{SOP})$ and $U(P_{TOP})$, respectively. The black dashed lines in Fig. 6 correspond to the estimated uncertainty of the piston gauge, $U(P_{PG})$.

The highest pressure in this work (25 kPa) is within the calculated uncertainties, while some of the lower ones are not. The data also show that there is a trend in the data, with the lower pressures diverging more from the estimated piston gauge pressure than the higher. This trend needs further investigation, but presently, we attribute it to a nonlinearity in the piston gauge, viz., a transition between the molecular and viscous flow in the piston cylinder gap, which causes a change in the effective area of the piston gauge.[44]

V. SUMMARY AND CONCLUSIONS

It has previously been shown that refractometers based on GAs MOdulation Refractometry (GAMOR), due to their extraordinary abilities to mitigate the influence of fluctuations and drifts,[26,27] are capable of providing high-precision (sub-ppm) assessments.[18,28–30] This has also allowed for the realization of transportable systems.[31,32]

This work presents a characterization of two Invar-based DFPC refractometers utilizing the GAMOR methodology, one stationary (SOP) and one transportable (TOP), for their ability to realize the pascal. The main aim of the work is to provide a first assessment of their expanded uncertainty regarding assessment of pressure of N_2 in the 4–25 kPa range. In addition to this, it serves the purpose of identifying their remaining shortcomings, which will be addressed in future developmental works with the aim of realizing refractometers with improved performance.

Although the two refractometers utilize the same procedure for regulation of the temperature of the experimental system (which is done by the use of Pt-100 sensors placed in drilled holes in the cavity spacer), they differ by the means they assess the temperature of the gas. While the TOP utilizes the Pt-100 sensors, the SOP assesses, for improved accuracy, the temperature by the use of a thermocouple with respect to a gallium fixed point cell.

The two refractometers were first individually characterized. The cavity deformations were assessed by the use of the methodology presented in Ref. 34. The uncertainty budget that resulted from the characterization, which is given in Table II, reveals an expanded uncertainty for assessment of pressure (k = 2) by the SOP and the TOP of $[(10\ \text{mPa})^2 + (10 \times 10^{-6}\ \text{P})^2]^{1/2}$ and $[(16\ \text{mPa})^2 + (28 \times 10^{-6}\ \text{P})^2]^{1/2}$, respectively. While the uncertainty of the SOP is mainly limited by the uncertainty in the molar polarizability of nitrogen (8 ppm), the uncertainty of the TOP is dominated by the temperature assessment (26 ppm). It was concluded that the total uncertainties of both refractometers were smaller than that of the piston gauge, which was assessed to $[(60\ \text{mPa})^2 + (41 \times 10^{-6}\ \text{P})^2]^{1/2}$.

The refractometers were thereafter compared over a period of 5 months at various pressures in the 4–25 kPa range both with each other and with the piston gauge. As is shown in Fig. 5, the comparison of the two refractometers revealed that, over the time of the campaign, which comprised four sets of data, taken during the months of October, November, December (2020), and February (2021), all measurements were within the calculated uncertainty for comparative measurements, which was 27 ppm (mainly attributed to the uncertainty in the temperature assessment of the TOP). This verified that the estimated error budgets for the uncorrelated errors hold over this length of time. It was also found that the spreads within each set of measurements were smaller than the spread of the entire set of data. This was attributed to long-term drifts in the temperature assessing Pt-100 probes in the TOP.

The comparison of the refractometers to the piston gauge showed that the pressure assessed with the refractometers jointly and consistently diverged from the calculated set pressure of the piston gauge and more so for the lower pressures than the highest. While these effects need further investigation, we currently attribute it to a change in the effective piston area of the piston gauge. The effective area of the piston had been calibrated by cross floating the piston gauge in the gauge mode, i.e., at atmospheric pressures. Under such conditions, there will be a contribution to the effective piston area from the drag force from the laminar flow through the cylinder piston gap. Since we in this work operate the piston gauge in an absolute mode, the pressures will be lower, resulting in a transition from a viscous to molecular flow through the cylinder piston gap. The contribution of this effect to the assessment of pressure has not been assessed for the particular piston gauge used in this work. However, it has been reported for a similar piston gauge that this effect is in the order of 50 ppm.[44] Hence, it is plausible that the main part of the discrepancy between the pressure assessments of the refractometers and those of the piston gauge (in particular, those at the lowest pressures) is due to this effect.

It can finally be concluded that the expanded uncertainty of the SOP is similar to that given by NIST for their highly stabilized ultralow expansion glass-based refractometer system, which is claimed to be $[(2.0\ \text{mPa})^2 + (8.8 \times 10^{-6}\ \text{P})^2]^{1/2}$,[25] which likewise is predominately limited by the uncertainty in the molar polarizability of nitrogen for kPa pressures. This shows that the GAMOR methodology performed in an Invar-based DFPC-refractometer is

capable of obtaining a realization of the pascal that is similar to what has been obtained by the so far most sophisticated refractometer system.

The results presented in this work will serve as the basis for further development of the refractometers. One of the goals of this developmental work will be to address higher pressures.

ACKNOWLEDGMENTS

This project (QuantumPascal, 18SIB04) has received funding from the EMPIR program co-financed by the Participating States and from the European Union's Horizon 2020 research and innovation program; Vetenskapsrådet (VR) (Nos. 621-2015-04374 and 621-2019-04159); the Umeå University Industrial doctoral school; the Vinnova Metrology Programme (Nos. 2017-05013, 2018-04570, and 2019-05029); and the Kempe Foundations (No. 1823.U12). The authors would like to thank Jonas Ågren at Lantmäteriet for providing the interpolated gravity value used in this work.

DATA AVAILABILITY

The data that support the findings of this study are available within the article.

REFERENCES

[1]C. R. Tilford, Metrologia **30**, 545 (1994).
[2]S. Semenoja and M. Rantanen, Vacuum **73**, 269 (2004).
[3]J. H. Hendricks and D. A. Olson, Measurement **43**, 664 (2010).
[4]J. W. Schmidt, K. Jain, A. P. Miiller, W. J. Bowers, and D. A. Olson, Metrologia **43**, 53 (2006).
[5]J. Ricker, J. Hendricks, T. Bock, D. Pražák, T. Kobata, J. Torres, and I. Sadkovskaya, Metrologia **54**, 07002 (2017).
[6]M. Stock, R. Davis, E. de Mirandés, and M. J. T. Milton, Metrologia **56**, 022001 (2019).
[7]M. Stock, R. Davis, E. de Mirandés, and M. J. T. Milton, Metrologia **56**, 049502 (2019).
[8]A. D. Buckingham and C. Graham, R. Soc. Lond. A **337**, 275 (1974).
[9]M. Jaeschke, H. M. Hinze, H. J. Achtermann, and G. Magnus, Fluid Phase Equilib. **62**, 115 (1991).
[10]H. J. Achtermann, G. Magnus, and T. K. Bose, J. Chem. Phys. **94**, 5669 (1991).
[11]P. F. Egan, J. A. Stone, J. H. Hendricks, J. E. Ricker, G. E. Scace, and G. F. Strouse, Opt. Lett. **40**, 3945 (2015).
[12]K. Jousten *et al.*, Metrologia **54**, S146 (2017).
[13]Y. Yang and T. Rubin, J. Phys: Conf. Ser. **1065**, 162003 (2018).
[14]Y. Takei, K. Arai, H. Yoshida, Y. Bitou, S. Telada, and T. Kobata, Measurement **151**, 107090 (2020).
[15]D. Mari, M. Bergoglio, M. Pisani, and M. Zucco, Meas. Sci. Technol. **25**, 125303 (2014).
[16]Z. Silvestri, D. Bentouati, P. Otal, and J-P. Wallerand, Acta IMEKO **9**, 305 (2020).
[17]M. Andersson, L. Eliasson, and L. R. Pendrill, Appl. Opt. **26**, 4835 (1987).
[18]I. Silander, C. Forssén, J. Zakrisson, M. Zelan, and O. Axner, Opt. Lett. **45**, 2652 (2020).
[19]EURAMET, see: https://www.euramet.org/research-innovation/search-research-projects/details/project/towards-quantum-based-realisations-of-the-pascal/ for "Towards Quantum-Based Realisations of the Pascal."
[20]H. Fang, A. Picard, and P. Juncar, Rev. Sci. Instrum. **73**, 1934 (2002).
[21]L. R. Pendrill, Metrologia **41**, S40 (2004).
[22]J. A. Stone and A. Stejskal, Metrologia **41**, 189 (2004).
[23]P. Egan and J. A. Stone, Appl. Opt. **50**, 3076 (2011).
[24]I. Silander, M. Zelan, O. Axner, F. Arrhén, L. Pendrill, and A. Foltynowicz, Meas. Sci. Technol. **24**, 105207 (2013).
[25]P. F. Egan, J. A. Stone, J. E. Ricker, and J. H. Hendricks, Rev. Sci. Instrum. **87**, 053113 (2016).
[26]O. Axner, I. Silander, C. Forssén, J. Zakrisson, and M. Zelan, J. Opt. Soc. Am. B. **37**, 1956 (2020).
[27]O. Axner, I. Silander, C. Forssén, J. Zakrisson, and M. Zelan, "Ability of gas modulation to reduce the pickup of drifts in refractometry" (submitted) (2021).
[28]I. Silander, T. Hausmaninger, M. Zelan, and O. Axner, J. Vac. Sci. Technol., A **36**, 03E105 (2018).
[29]I. Silander, T. Hausmaninger, C. Forssén, M. Zelan, and O. Axner, J. Vac. Sci. Technol., B **37**, 042901 (2019).
[30]M. Zelan, I. Silander, C. Forssén, J. Zakrisson, and O. Axner, Acta IMEKO **9**, 299 (2020).
[31]C. Forssén, I. Silander, D. Szabo, G. Jönsson, M. Bjerling, T. Hausmaninger, O. Axner, and M. Zelan, Acta IMEKO **9**, 287 (2020).
[32]C. Forssén, I. Silander, O. Axner, and M. Zelan, "Short term performance of two independent GAMOR based refractometers for assessment of pressure" (submitted) (2021).
[33]I. Silander, C. Forssén, J. Zakrisson, M. Zelan, and O. Axner, Acta IMEKO **9**, 293 (2020).
[34]J. Zakrisson, I. Silander, C. Forssén, M. Zelan, and O. Axner, J. Vac. Sci. Technol., B **38**, 054202 (2020).
[35]O. Axner, I. Silander, T. Hausmaninger, and M. Zelan, "Drift-free Fabry-Perot-cavity-based optical refractometry—Accurate expressions for assessments of gas refractivity and density," arXiv:1704.01187v2 (2017).
[36]P. F. Egan, J. A. Stone, J. K. Scherschligt, and A. H. Harvey, J. Vac. Sci. Technol., A **37**, 031603 (2019).
[37]The gallium cell was run in an automated mode of operation in a series of recurrent freezing and melting cycles. Each measurement series was started by resetting the cell (i.e., freezing the gallium). During the subsequent heating cycles, the melting plateau was reached after 4 h after which temperature measurements commenced. When the temperature of the cell increased noticeably (which took place when a large part of the gallium had melted after ≈100 h), the system initiated automatically a new freezing process.
[38]The assessment of the cavity deformation could be done with a minimum of measurement uncertainty. However, the procedure used assumed access to pure gases (He and N_2). It is not unambiguously ruled out that, at the time of assessment of the deformation presented in this work, the gas supplies (of gases) were exposed to finite degrees of contamination. Due to the low refractivity of helium, the determination of cavity deformation is particularly sensitive to contamination of the helium supply. Any contamination of the helium supply will result in an overestimation of the cavity deformation. Throughout the campaign, this measurement was, therefore, repeated with three different supplies of helium: one 10 l cylinder of 6N He and two 10 l tubes of 7N He. We found that the assessed deformation increased slightly after each switch of the gas cylinder. Although no dedicated study of the cause of this was made in this work, we tentatively attribute this to contamination of the He gas. This indicates that the system, as used when the above-mentioned characterization was performed, potentially was affected by an incomplete evacuation of ambient air from the gas system following changes of gas cylinders. Means to eliminate this effect is under way.
[39]M. Puchalski, K. Piszczatowski, J. Komasa, B. Jeziorski, and K. Szalewicz, Phys. Rev. A **93**, 032515 (2016).
[40]E. R. Peck and B. N. Khanna, J. Opt. Soc. Am. **56**, 1059 (1966).
[41]B. Baker, Am. J. Phys. **67**, 712 (1999).
[42]K. Jousten, Vacuum **45**, 1205 (1994).
[43]T. Rubin *et al.*, "Thermodynamic effects in a gas modulated Invar-based dual Fabry-Pérot cavity refractometer" (unpublished) (2021).
[44]K. Jain, W. Bowers, and J. W. Schmidt, J. Res. Natl. Inst. Stand. Technol. **108**, 135 (2003).